[CANCER RESEARCH 62, 2203–2209, April 15, 2002]

Advances in Brief

Identification of the p33^{ING1}-regulated Genes that Include *Cyclin B1* and Proto-oncogene *DEK* by Using cDNA Microarray in a Mouse Mammary Epithelial Cell Line NMuMG[1]

Masato Takahashi, Naohiko Seki, Toshinori Ozaki, Masaki Kato, Tomoko Kuno, Takahito Nakagawa, Ken-ichi Watanabe, Koh Miyazaki, Miki Ohira, Shunji Hayashi, Mitsuchika Hosoda, Hisashi Tokita, Hiroyuki Mizuguchi, Takao Hayakawa, Satoru Todo, and Akira Nakagawara[2]

Division of Biochemistry [M. T., T. O., T. K., T. N., K. W., K. M., M. O., S. H., M. H., A. N.] and Division of Animal Science [H. T.], Chiba Cancer Center Research Institute, Chuoh-ku, Chiba 260-8717; Department of General Surgery, Hokkaido University School of Medicine, Kita-ku, Sapporo 060-8638 [M. T., T. N., K. W., S. H., M. H., S. T.]; Department of Functional Genomics, Chiba University Graduate School of Medicine, Chuo-ku, Chiba 260-8670 [N.S., M.K.]; and Division of Biological Chemistry and Biologicals, National Institute of Health Science, Kamiyoga, Setagaya-ku, Tokyo 158-8501 [H. M., T. H.], Japan

Abstract

The candidate tumor suppressor p33^{ING1} plays an important role in inducing growth arrest at G_0-G_1 phase of the cell cycle and/or promoting apoptosis in cancerous cells. p33^{ING1} is reported to act as a transcriptional cofactor by associating with tumor suppressor p53, HAT, or histone deacetyltransferase, suggesting that p33^{ING1} is involved in chromatin-mediated transcriptional regulation. However, the molecular mechanism of p33^{ING1}-mediated transcriptional regulation is poorly understood. Here we analyzed expression profiles in mouse mammary epithelial cells (NMuMG) by using a cDNA microarray consisting of 2304 mouse cDNAs after inducing transformation with antisense inhibitor of growth 1 (*ING1*) in retrovirus vector. The subsequent confirmation of the altered expression levels of the selected genes by semiquantitative reverse transcription-PCR demonstrated that overexpression of the antisense *ING1* stimulated expression of 14 genes, which included *cyclin B1*, 12-*O*-tetradecanoylphorbol-13-acetate-*inducible sequence 11*, proto-oncogene *DEK*, and *osteopontin*, whereas we have detected transcriptional repression of 5 genes, including *TPT1*. In addition, adenovirus-mediated overexpression of ING1 in NMuMG cells resulted in down-regulation of *cyclin B1*, 12-*O*-tetradecanoylphorbol-13-acetate-*inducible sequence 11*, *DEK*, and *osteopontin*, whereas the levels of *TPT1* expression were increased. The further analysis using p53$^{-/-}$ SAOS2 cells showed that the p33^{ING1}-induced *cyclin B1* down-regulation was p53 dependent. Thus, our cDNA microarray analysis suggested that p33^{ING1} targets the multiple genes, including proto-oncogene *DEK* and *cyclin B1*, at least some of which are regulated in a p53-dependent manner, in the cells undergoing cell growth or apoptosis.

Introduction

A novel candidate tumor suppressor *ING1*[3] has been identified using a positive selection procedure that combined a PCR-mediated subtractive hybridization of cDNAs derived from normal and cancer cells with an *in vivo* selection assay (1). *ING1* mRNA is expressed ubiquitously in adult mouse tissues, whereas its expression levels varied among them (2). ING1 is present in at least three variants (p47^{ING1a}, p33^{ING1b}, and p24^{ING1c}) arising from the differential initiation and the splicing of mRNAs (2, 3). These ING1 variants share the nuclear localization signal, as well as the evolutionarily conserved PHD finger domain, which has been found in various transcription factors and proteins involved in chromatin-mediated transcriptional regulation (4). ING1 was also reported to be associated with HAT activity (5) or histone deacetyltransferase-dependent transcriptional repression, indicating that ING1 is involved in chromatin remodeling (6).

Inhibition of endogenous *ING1* expression by antisense RNA results in the anchorage-independent growth in soft agar medium and promotes the tumor formation in nude mice (1). In addition, forced expression of antisense RNA prolongs the proliferative life span of normal human fibroblasts (7). Conversely, ectopic overexpression of *ING1* leads to the G_0-G1 arrest of the cell cycle or apoptosis in different experimental systems (1, 8). Accordingly, the levels of *ING1* expression are regulated in a cell cycle-dependent manner and are also increased during the serum starvation-induced apoptosis in mouse teratocarcinoma cells (7, 8). In addition, decreased expression of *ING1* was observed in cells of several breast carcinomas and gliomas (9, 10). Intriguingly, ING1 was physically associated with tumor suppressor p53 and activated p53-mediated transcriptional activation and growth suppression (10, 11). These observations suggest that ING1 contributes to the regulatory mechanism of cell cycle progression, cellular aging, and apoptosis.

ING1 has been mapped to human chromosome 13q33-34, which is the locus for the candidate tumor suppressor gene(s) of various human cancers (9, 12–15). As reported previously, the *ING1* gene was rearranged in a neuroblastoma cell line, SK-N-SH, generating a truncated gene product (1). Several missense mutations have been reported in primary esophageal squamous cell cancers and head and neck squamous cell carcinomas (3, 16). Those mutations were detected within the nuclear localization signal or the PHD finger domain of ING1, indicating that normal function of ING1 may be abrogated in some of those cases. However, the frequency of *ING1* mutation was quite low in these tumors, and no mutations were detected in breast and ovarian cancers (3, 9, 16). Thus, it is still unclear whether or not ING1 could act as a classic Knudsen-type tumor suppressor.

In the present study, we analyzed expression profiles of 2304 genes by using cDNA microarray in mouse mammary epithelial cells (NMuMG) after antisense *ING1*-induced transformation. The subse-

Received 10/3/01; accepted 2/26/02.

The costs of publication of this article were defrayed in part by the payment of page charges. This article must therefore be hereby marked *advertisement* in accordance with 18 U.S.C. Section 1734 solely to indicate this fact.

[1] Supported in part by a Grant-in-Aid from the Ministry of Health and Welfare for a New 10-Year Strategy of Cancer Control, a Grant-in-Aid for Scientific Research on Priority Areas, and a Grant-in-Aid for Scientific Research (B) from the Ministry of Education, Culture, Sports, Science and Technology, Japan. M. T. and K. M. are awardees of the Research Resident Fellowship from the Foundation for Promotion of Cancer Research in Japan.

[2] To whom requests for reprints should be addressed, at Division of Biochemistry, Chiba Cancer Center Research Institute, 666-2 Nitona, Chuoh-ku, Chiba 260-8717, Japan. Phone: 81-43-264-5431; Fax: 81-43-265-4459; E-mail: akiranak@chiba-ccri.chuo.chiba.jp.

[3] The abbreviations used are: ING1, inhibitor of growth 1; *RP*, ribosomal protein; RT-PCR; reverse transcription-PCR; HDAC, histone deacetylase; GSE, genetic suppressor element; MOI, multiplicity of infection; EST, expressed sequence tag; *TIS11*, 12-*O*-tetradecanoylphorbol-13-acetate-*inducible sequence 11*; AFP, *α-fetoprotein*; *TPT1, translationally controlled 1*; TPA, 12-*O*-tetradecanoylphorbol-13-acetate; *TDE1, testicular tumor differentially expressed 1*; HAT, histone acetyltransferase; IGF-II, insulin-like growth factor-II; GAPDH, glyceraldehyde-3-phosphate dehydrogenase; *SDR, testicular tumor differentially expressed*.

quent confirmation of the candidate target genes by semiquantitative RT-PCR identified 14 and 5 genes whose expression levels were up- and down-regulated by overexpression of antisense *ING1*, respectively. Furthermore, adenovirus-mediated overexpression of sense *ING1* in NMuMG cells confirmed the target genes that included *cyclin B1* and proto-oncogene *DEK*.

Materials and Methods

Cell Culture. NMuMG (mouse epithelial cell line from mammary gland) cells, NIH3T3 cells, and human osteosarcoma SAOS2 cells were grown in DMEM with 10% (volume for volume) heat-inactivated fetal bovine serum in the presence of 100 units/ml penicillin and 100 μg/ml streptomycin. Cells were maintained under an atmosphere of 5% CO_2 at 37°C.

GSE Method. GSE assay was performed as described previously (1). In brief, a cDNA fragment encoding a COOH-terminal region of ING1 was amplified by PCR-based strategy and subcloned into the *Hpa*I restriction site of the pLXSN vector in an antisense orientation to give pLXSN-antisense *ING1*. pLXSN or pLXSN-antisense *ING1* was transfected into the φ2 packaging cells, and NMuMG cells (1×10^6 cells) infected with virus-containing culture medium were injected into the lateral subcutis of athymic nude mice. The sequence of 388 bp for antisense *ING1* was designed to block all isoforms at the region, including the PHD finger domain within exon 2 as follows: 5′-gagtttagtccccctcctcccgcaagaaatcagtctgagacttaagtgttgaatcaaacctatatttgtagtttctaaaatgctgatccacagaccactttcttgttacacgtgtaccaatgaaaacaaaaggcaaacagaatcactgccatccctatgaaaggaatggttccttttctaacattctttaaaaatatacattttacactccttgcacctcacacaaaggcagcaatgtaataaatacacggtttattttgtcctcctcacaccaggcgcctgtccacaaactacctgttgtaagccctctctttttttggatttctccagggctttgtccatggtcttctcgttctccccccggcacttgggacagtaccacttgccctt-3′.

Soft Agar Colony Growth Assay. NMuMG cells (5×10^4 cells) infected with pLXSN or pLXSN-antisense *ING1* were suspended in 3 ml of 0.4% low melting point agarose (SeaPlaque; FMC Bioproducts, Rockland, ME) dissolved in culture medium and plated onto an agarose bed consisting of 0.8% low melting point agarose and the same medium. After 5 weeks, the number of visible colonies >100 μm was counted.

Focus Forming Assay. NIH3T3 cells (5×10^4 cells) infected with pLXSN or pLXSN-antisense *ING1* were seeded and maintained in culture medium containing 5% (volume for volume) heat-inactivated fetal bovine serum for 4 weeks. Cells were then fixed in methanol, and the number of foci was scored.

Generation of Recombinant Adenoviral Vector. For construction of the adenovirus expression vector, a full-length *ING1* cDNA or the *Hin*dIII-*Xba*I restriction fragment derived from pcDNA3-*p53* was filled in with Klenow fragment and inserted into the enzymatically modified *Not*I site of the shuttle vector pHMCMV6 (17, 18). The resultant shuttle vector was digested with I-CeuI and PI-SceI and subcloned into the identical restriction sites of the adenovirus expression vector pAdHM4. The recombinant adenovirus construct was introduced into human embryonic kidney 293 cells.

RNA Isolation and RT-PCR Analysis. Total RNA was prepared using Trizol reagent (Life Technologies, Inc., Rockville, MD) according to the manufacturer's protocol. cDNA was generated from 5 μg of total RNA using Moloney murine leukemia virus reverse transcriptase (SuperScript II; Life Technologies, Inc.). RT-PCR amplification was carried out for one cycle of 95°C for 2 min, followed by 25 cycles of 95°C for 30 s, 58°C for 30 s, and 72°C for 30 s. PCR primers used were as follows: *serum albumin*, 5′-AACTATGCTGAGGCCAAGGA-3′ (sense) and 5′-CTGAGGTGCTTTCTGGGTGT-3′ (antisense); *AFP*, 5′-AAAGCTGCGCTCTCTACCAG-3′ (sense) and 5′-GGTGATGCATAGCCTCCTGT-3′ (antisense); *aldehyde dehydrogenase II*, 5′-CGGATTTAGGAGGCTGCATA-3′ (sense) and 5′-AATGTTTACCACGCCAGGAG-3′ (antisense); *cyclin B1*, 5′-ATCGGGGAACCTCTGATTTT-3′ (sense) and 5′-TCACACACAGGCACCTTCTC-3′ (antisense); *TIS11*, 5′-AATGCCATGGCTTCTAAGGA-3′ (sense) and 5′-AATGGCAGTGGAAAATCCAA-3′ (antisense); *DEK*, 5′-AGGAGGAAGAGGACGAGGAC-3′ (sense) and 5′-GGAAAGCCACTGAACTGACC-3′ (antisense); *osmotic stress protein*, 5′-GGATCCTGCTGAAATGGAAA-3′ (sense) and 5′-TGTGCTGTGAGCTTCCTTTG-3′ (antisense); *IGF-II receptor*, 5′-TGCACCATGTCTTTGTAGGC-3′ (sense) and 5′-ACTAGGCCTGGCTTGAGCTT(antisense); *myosin light chain*, 5′-GAACAGGGATGGCATTATCG-3′ (sense) and 5′-TTGATCTCCTCCTGGGAAAA-3′ (antisense); *SDR* gene, 5′-GGTTTCTCCCCTCTCCTTTG-3′ (sense) and 5′-ACTCTCATAGCGCACCTGCT3′ (antisense); *osteopontin*, 5′-TCTGATGAGACCGTCACTGC-3′ (sense) and 5′-TGGTTCATCCAGCTGACTTG-3′ (antisense); *EST-3*, 5′-TGGGAGACCAGTGAAAGCAC-3′ (sense) and 5′-ACCCTTGGCCTGGTTTTTAC-3′ (antisense); *EST-4*, 5′-GCCATACGGCTGGATAGGTA-3′ (sense) and 5′-AAGGCCCAGAAGGCATAAGT-3′ (antisense); γ *actin*, 5′-GTGCTATGTTGCCCTGGATT-3′ (sense) and 5′-CTTCTGCATCCTGTCAGCA-3′ (antisense); *TDE1*, 5′-GACCCTCTCTGGGAGTGACA-3′ (sense) and 5′-GGAGCCACAAGAGTCCAGAG-3′ (antisense); ζ *proteasome*, 5′-GAGAGTGTGACCCAGGCTGT-3′ (sense) and 5′-GCTTCTCCTCCATGACTTGC-3′ (antisense); *EST-1*, 5′-TTGCACCTGCACATACACCT-3′ (sense) and 5′-TGTTGCCTTTGACCAGATGA-3′ (antisense); *RP S11*, 5′-TAACGTCTCCATCCGAGGTC-3′ (sense) and 5′-GGCCAGAGTCCCCTTAGAAC-3′ (antisense); *elongation factor-2*, 5′-TGTCCAAGTCCCCCAATAAG-3′ (sense) and 5′-AGAGCGCCCTCCTTAGTAGC-3′ (antisense); *RP S7*, 5′-ACGAGTTCGAGTCTGGCATC-3′ (sense) and 5′-GCGCTTCTGCTTATTTTTCG-3′ (antisense); *EST-2*, 5′-CAGGCTCCTCTCCATATCCA-3′ (sense) and 5′-AAAAACAACGGAAAGGAGCA-3′ (antisense); *TPT1*, 5′-TGGAGCTGCAGAGCAGATTA-3′ (sense) and 5′-ACAATGCCACCACTCCAAAT-3′ (antisense); *RP S29*, 5′-CTGAAGGCAAGATGGGTCAC-3′ (sense) and 5′-CATGATCGGTTCCACTTGGT-3′ (antisense); *int-6*, 5′-TCAGGCAGAAACAGAACCAA-3′ (sense) and 5′-TGCATCCCAATTCTGCATTA-3′ (antisense); *RP L12*, 5′-CAGAACAGACAGGCCCAGAT-3′ (sense) and 5′-CACTCCACTGCACCACTGTT-3′ (antisense); *p21^{WAF1}*, 5′-GTCCAATCCTGGTGATGTCC-3′ (sense) and 5′-CAGGGCAGAGGAAGTACTGG-3′ (antisense); *GAPDH*, 5′-ACCTGACCTGCCGTCTAGAA-3′ (sense) and 5′-TCCACCACCCTGTTGCTGTA-3′ (antisense); human *cyclin B1*, 5′-TGTGGATGCAGAAGATGGAT-3′ (sense) and 5′-AAACATGGCAGTGACACCAA-3′ (antisense); and human *GAPDH*, 5′-ACCTGACCTGCCGTCTAGAA-3′ (sense) and 5′-TCCACCACCCTGTTGCTGTA-3′ (antisense). After the final cycle, we used a 4-min extension period at 72°C. The PCR products were analyzed by gel electrophoresis on 2% agarose gels, stained with ethidium bromide, and visualized on the UV transilluminator.

cDNA Microarray Analysis. A cDNA array with 2304 cDNAs derived from mouse fetus (a kind gift from T. Hashimoto) was prepared as described previously (19). Each slide carried mouse β-actin cDNA to normalize the intensity of signals. For the preparation of fluorescent probes, 2 μg of poly(A)$^+$RNA purified from NMuMG cells infected with pLXSN or pLXSN-antisense *ING1* were incubated with 4.5 μg of oligodeoxythymidylate primer (in a total volume of 15.4 μl) at 70°C for 10 min and chilled on ice. Then we added 6 μl of 5 × SuperScript II buffer, 3 μl of 100 mM DTT, 0.6 μl of deoxynucleotide triphosphate mixture (25 mM dATP, dCTP, dGTP, and 10 mM dTTP), 3 μl of 1 mM Cy3- (mRNA from pLXSN-antisense *ING1*-infected cells) or Cy5- (mRNA from empty vector-infected cells) dUTP, and 400 units of SuperScript II. After the incubation at 42°C for 1 h, template mRNAs were degraded at 65°C for 10 min in the presence of 1.5 μl of 1N NaOH/20 mM EDTA and then neutralized with 270 μl of TE (pH 8.0) and 1.5 μl of 1N HCl. Hybridization was performed in a solution containing 2 mg/ml yeast RNA (Sigma Chemical Co., St. Louis, MO), 2 mg/ml poly(A) (Roche, Basel, Switzerland), 3.4 × SSC, and 0.3% SDS at 65°C overnight under humidified condition. After the hybridization, the arrays were washed twice for 5 min with 2 × SSC/0.1% SDS at room temperature, twice for 5 min with 0.2 × SSC/0.1% SDS at 40°C, and finally rinsed with 0.2 × SSC. The arrays were centrifuged at 1000 rpm for 1 min and then scanned with a fluorescence laser-scanning device (ScanArray4000; GSI Lumonics).

Western Analysis. Total cell lysates were separated on a 10% SDS-polyacrylamide gel and electrotransferred onto a nitrocellulose membrane. The membrane was probed with a monoclonal antibody against ING1 (kindly provided by K. Riabowol). The membrane was visualized with an enhanced chemiluminescence detection system (enhanced chemiluminescence; Amersham Pharmacia Biotech, Piscataway, NJ).

Results

Growth-inhibitory Activity of ING1. To identify genes involved closely in ING1-induced growth and/or tumor suppression, we decided to use the mouse breast epithelial cell system (NMuMG cells). Consistent with the previous report (1), NMuMG cells infected with the recombinant retrovirus vector for the antisense *ING1* cDNA

(pLXSN-antisense *ING1*) strongly inhibited expression of ING1 proteins (Fig. 1*A*) and promoted the anchorage-independent growth in soft agar medium, compared with cells infected with the empty vector (pLXSN; Fig. 1*B*). Similarly, down-regulation of *ING1* expression by the antisense construct increased the frequency of focus formation in NIH3T3 cells (Fig. 1*C*). To examine the effect of antisense *ING1* on the tumorigenicity, NMuMG cells infected with the pLXSN-antisense *ING1* or the pLXSN were injected s.c. into nude mice. Eight weeks after the injection, four of the five animals injected with cells expressing antisense *ING1* carried tumors, whereas only one of the five animals with control cells developed a small tumor (Fig. 1*D*). Thus, our system appeared to be suitable to search for the ING1-regulated genes.

Gene Expression Analysis by cDNA Microarray. We performed the expression analyses of 2304 genes in NMuMG cells infected with pLXSN-antisense *ING1* by means of cDNA microarray. The cDNA probes derived from NMuMG cells infected with pLXSN-antisense *ING1* or the empty vector were fluorescently labeled with Cy3-dUTP (red) or Cy5-dUTP (green), respectively. These probes were applied simultaneously onto the microarray, and the two fluorescent images were scanned with a fluorescence laser-scanning device. Each signal was normalized so that the Cy3:Cy5 intensity ratio of the housekeeping gene (β-actin) signal was 1. Red and green fluorescent signals indicated genes whose expression levels were relatively higher in cells infected with pLXSN-antisense *ING1* and the backbone vector, respectively. Yellow signals indicate genes with equal expression in both cells. In the present study, we considered genes that exhibited a Cy3:Cy5 ratio > 1.5 as candidates of up-regulated genes and those with a Cy3:Cy5 ratio < 0.67 as candidates of down-regulated genes. Fig. 2*A* shows the scatter plots of the average mRNA expression of 2304 genes. Table 1 lists the genes that have shown a $\geq$1.5-fold increase or decrease in expression level in at least three of four independent experiments. Sixteen (0.7%) and 9 (0.4%) genes displayed relatively higher and lower expression levels during the antisense *ING1*-induced transformation, respectively. Each of the up- and down-regulated genes included two ESTs. Fig. 2*B* shows a representative result of microarray detection. *Serum albumin, aldehyde dehydrogenase II, cyclin B1, TIS11,* and proto-oncogene *DEK* displayed red signals, whereas *RP S29* and *TPT1* showed green signals. *Serum albumin, AFP,* and *aldehyde dehydrogenase II* were induced by the antisense *ING1* to an extent that was 5.8, 5.4, and 2.8 times greater than the control infection, respectively, whereas *IGF-II receptor, myosin light chain, SDR* gene, and *TDE1* were slightly activated.

Semiquantitative RT-PCR Analysis. To examine the reliability of the expression changes detected by the profiling analysis using the cDNA microarray, the semiquantitative RT-PCR analysis with the same RNA samples that had served for the microarray analysis was performed. In agreement with the microarray results, the expression

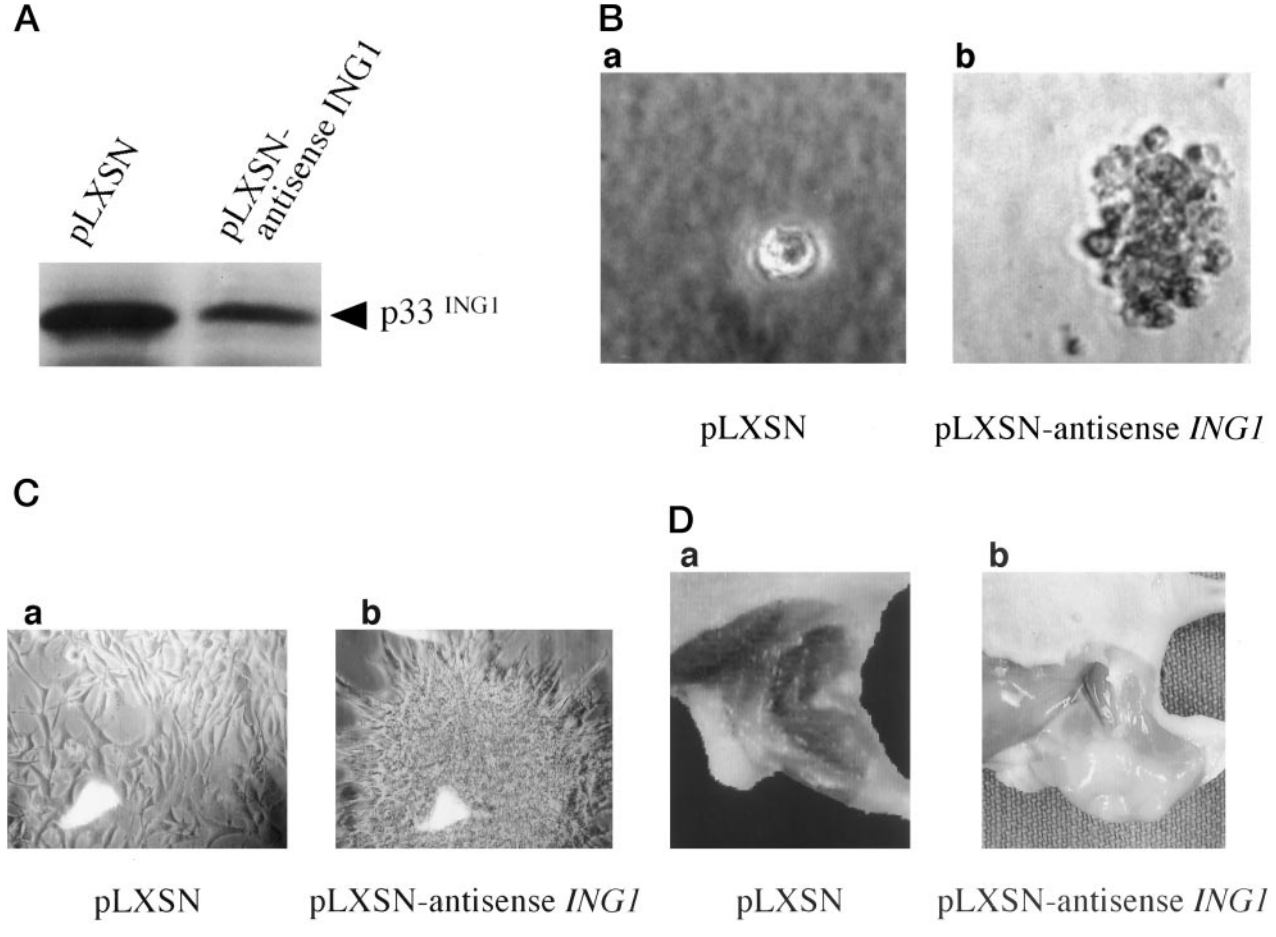

Fig. 1. Growth-inhibitory activity of ING1. *A,* decreased expression of the ING1 protein in NMuMG cells after stable infection by retrovirus vector carrying with antisense-*ING1*. Western blot analysis. *B,* soft agar colony formation assay. A total of 5×10^4 NMuMG cells was infected with pLXSN (*a*) or pLXSN-antisense *ING1* (*b*). After growth for 5 weeks in the soft agar medium, the number of colonies formed in soft agar was counted. Representative results are shown. *C, in vitro* focus formation. NIH3T3 cells (5×10^4 cells/10-cm dish) infected with pLXSN (*a*) or pLXSN-antisense *ING1* (*b*) were grown in DMEM containing 5% fetal bovine serum for 4 weeks. Cells were then fixed in methanol and photographed, and the number of foci was scored. Representative results are shown. *D,* tumor formation in nude mice. Six-week-old nude mice (BALB/c-*nu*/*nu*) were given injections of 1×10^6 NMuMG cells infected with pLXSN (*a*) or pLXSN-antisense *ING1* (*b*). Experiments were performed with five animals in each injection. Mice were examined for tumor formation over an 8-week period, and the representative cases are shown.

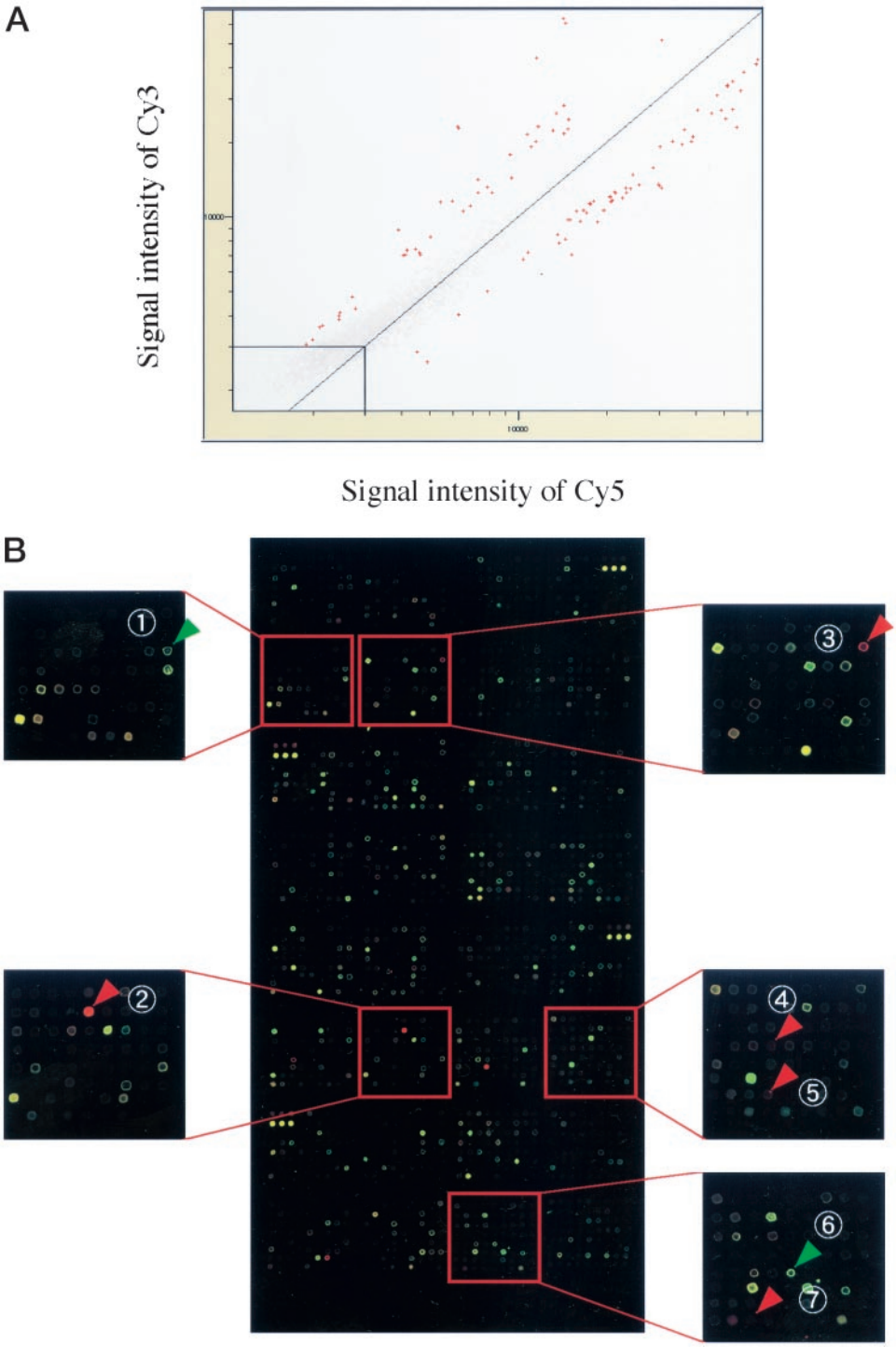

Fig. 2. Expression intensity in NMuMG cells infected with pLXSN-antisense *ING1* compared with those infected with empty pLXSN vector. *A*, representative scatter plots of cDNA microarray analysis. The cDNA microarray was hybridized with Cy3- or Cy5-labeled probe prepared from cells infected with pLXSN-antisense *ING1* or pLXSN, respectively. The expression levels were analyzed with the Quant Array computer program. The *red* spots in this graph represent genes whose expression levels changed >1.5-fold in at least three of four independent experiments. The axes scales are logarithmic. *B*, a representative cDNA microarray analysis. *Green* and *red* color represent genes whose expression levels were significantly down- and up-regulated in cells infected with pLXSN-antisense *ING1*, respectively. *Yellow* spots show equal expression in both cells. Graduated color patterns indicate the degrees of expression changes. *Spots 1–7, RP S29, serum albumin, aldehyde dehydrogenase II, cyclin B1, TIS11, TPT1,* and proto-oncogene *DEK*, respectively.

levels of 14 of 16 genes (87.5%), which were considered as up-regulated genes by the microarray analysis, were increased on antisense *ING1* overexpression (Fig. 3*A*). Among them, *cyclin B1, TIS11, DEK,* and *osteopontin* were induced strongly by antisense *ING1*. In addition, 56.7% (5 of 9 genes) was confirmed to be down-regulated by semiquantitative RT-PCR analysis, and the expression level of *TPT1* was reduced significantly (Fig. 3*B*).

Induction of the Selected Genes by Adenovirus-mediated Overexpression of ING1. In the cDNA microarray and in the semiquantitative RT-PCR analyses, we found that ING1 was the potent regulator of *cyclin B1, TIS11, DEK, osteopontin,* and *TPT1* expression. To examine whether the increase in *TPT1* level or the decrease in *cyclin B1, TIS11, DEK,* and *osteopontin* levels was dependent on ING1, the expression analysis was performed in NMuMG cells infected with recombinant adenovirus encoding ING1 (Ad-*ING1*). As shown in Fig. 4, total RNA and total cell lysate were prepared at the times indicated after the adenovirus infection at MOI of 10, and the semiquantitative RT-PCR and Western blotting were carried out. As described previously, because p53-mediated transactivation of $p21^{WAF1}$ promoter was dependent on ING1 (11), we also examined the expression level of $p21^{WAF1}$. Western analysis revealed that ING1 started to be accumulated at 6 h after the infection, reaching a maximum level at 48 h.

Initiation of the *p21*^{WAF1} transcription was slightly delayed (at 12 h after the infection) compared with that of ING1. We subsequently examined whether the overexpression of ING1 could affect the expression pattern of the selected genes. Consistent with the results obtained by the cDNA microarray followed by the semiquantitative RT-PCR, the endogenous level of *cyclin B1*, *TIS11*, and *DEK* mRNAs was strikingly reduced in a time-dependent manner by the forced expression of ING1. Of interest, the initiation of the transcriptional down-regulation of these genes (at 48 h after the infection) was delayed significantly compared with that of ING1 accumulation. Similar delayed patterns of down-regulation were observed in *osteopontin* expression; however, the extent of the reduction was relatively low. On the other hand, the accumulation of *TPT1* mRNA was detected at 18 h after the infection, slightly delayed compared with that of *p21*^{WAF1}. These results verified the reliability of our cDNA microarray analysis to identify genes that could be involved in ING1-mediated transcriptional regulation.

Table 1 *Genes of up- or down-regulated by overexpression of antisense ING1*

Gene	Fold change[a]			
	Exp. 1	Exp. 2	Exp. 3	Exp. 4
Serum albumin	4.44	7.13	4.30	7.21
AFP	4.19	7.84	4.54	5.02
Aldehyde dehydrogenase II	3.62	1.60	3.46	2.44
Cyclin B1	2.25	2.29	2.09	1.58
TIS11	2.11	3.09	1.97	1.70
DEK	1.70	1.84	1.55	1.92
Osomotic stress protein	1.61	2.05	1.73	1.76
IGF-II receptor	1.51	1.66	1.58	1.80
Myosin light chain	1.71	1.65	1.54	1.44
SDR	1.63	1.52	1.67	1.21
Osteopontin	1.68	3.03	1.41	3.42
EST-3	1.94	2.46	1.34	1.89
EST-4	1.65	1.73	1.40	2.57
γ actin	1.90	1.60	1.36	2.03
TDE 1	1.53	1.45	1.56	1.70
ζ proteasome	1.40	2.26	2.47	3.45
EST-1	0.66	0.52	0.57	0.60
RP S11	0.66	0.51	0.61	0.52
Ef-2 (*elongation factor-2*)	0.59	0.66	0.51	0.79
RP S7	0.52	0.61	0.57	0.77
EST-2	0.54	0.58	0.51	0.73
TPT1	0.55	0.70	0.52	0.66
RP S29	0.66	0.68	0.55	0.62
Int-6	0.68	0.65	0.60	0.63
RP L12	0.67	0.61	0.65	0.76

[a] Genes with a ≥1.5-fold difference in signal intensity between NMuMG cells infected with pLXSN and those with pLXSN-antisense *ING1* are presented. Fold change indicates a ratio of signal intensity (Cy3:Cy5).

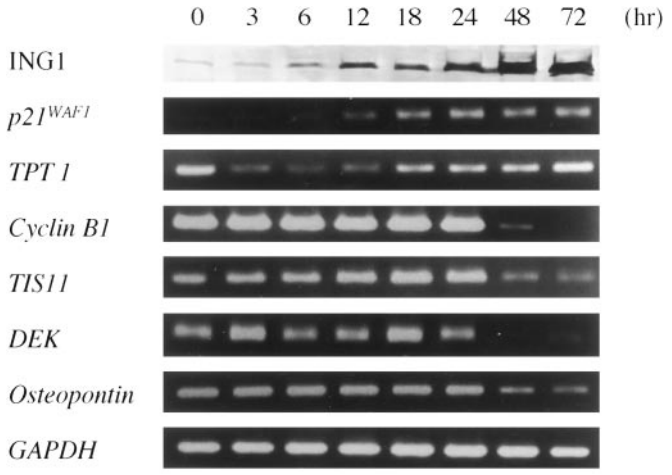

Fig. 4. Time course of *p21*^{WAF1}, *TPT1*, *cyclin B1*, *TIS11*, *DEK*, and *osteopontin* expression in NMuMG cells infected with recombinant adenovirus encoding ING1 (Ad-*ING1*). Cells were infected with 10 MOI of Ad-*ING1* and grown for the indicated time periods before RNA preparation. RT-PCR was carried out under linear amplification conditions. *GAPDH* expression is shown as a control. The expression level of ING1 was analyzed by Western blotting with a monoclonal anti-ING1 antibody.

ING1-induced Suppression of Cyclin B1 Is p53 Dependent. As described previously, ING1 cooperates directly with p53 by modulating p53-dependent transcription (10, 11). To examine whether the ING1-mediated down-regulation of *cyclin B1* expression was dependent on p53, p53-deficient SAOS2 cells were infected with recombinant adenovirus encoding ING1 (Ad-*ING1*) or ING1 and p53 (Ad-*p53*), and then the expression level of endogenous *cyclin B1* was measured by the semiquantitative RT-PCR. The expression of the transgenes was confirmed by both RT-PCR and Western blotting. As shown in Fig. 5, overexpression of *ING1* alone caused no significant

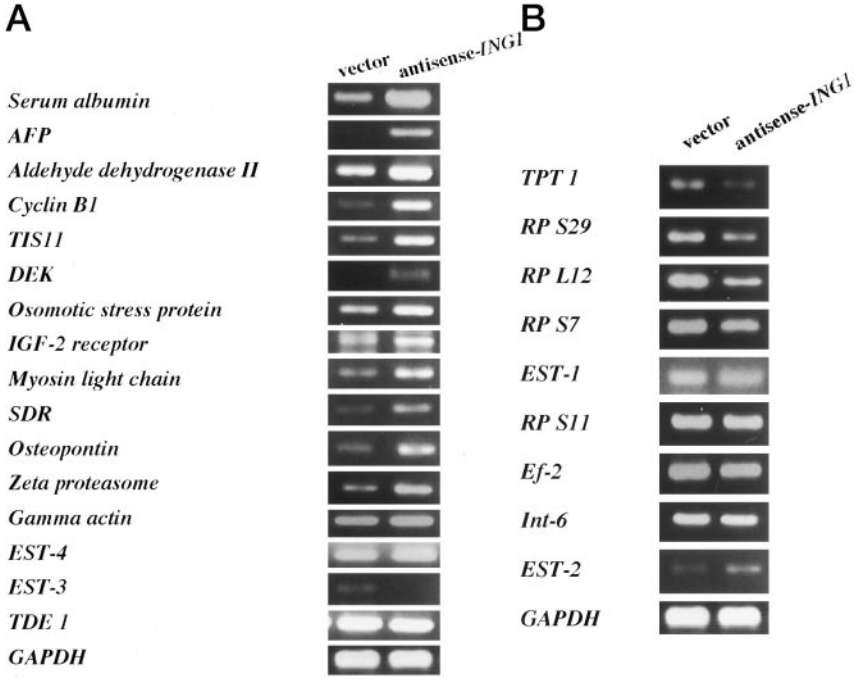

Fig. 3. Semiquantitative RT-PCR analysis using RNA from NMuMG cells infected with an empty vector or pLXSN-antisense *ING1*. *A*, genes with up-regulated expression in cells infected with pLXSN-antisense *ING1*. *B*, genes with down-regulated expression in cells infected with pLXSN-antisense *ING1*. *GAPDH* expression is shown as a control. GenBank accession nos. of *EST-1*, *EST-2*, *EST-3*, and *EST-4* are AI573918, X75312, AU080496, and AF111103, respectively.

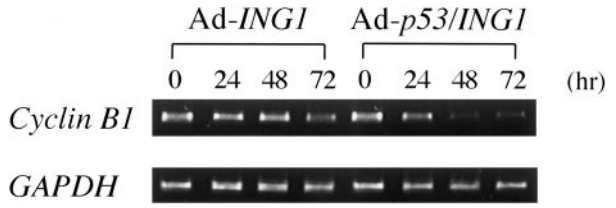

Fig. 5. ING1-mediated down-regulation of *cyclin B1* expression is p53 dependent. p53-deficient SAOS2 cells were infected with 30 MOI of Ad-*ING1* or Ad-*ING1* and Ad-*p53* and maintained for the indicated time periods before RNA preparation. Semiquantitative RT-PCR was performed using primers specific for *cyclin B1* under linear amplification conditions. *GAPDH* expression is shown as a control.

change in *cyclin B1* expression in SAOS2 cells. In contrast, a remarkable decrease in *cyclin B1* expression level was observed 48 h after the infection with both Ad-*ING1* and Ad-*p53*. Thus, it is likely that p53-dependent mechanism contributes to the down-regulation of *cyclin B1* expression by ING1. *DEK* also had a tendency to be down-regulated when both Ad-*ING1* and Ad-*p53* were infected into SAOS2 cells (data not shown).

Discussion

A cDNA microarray technology has been shown to be a powerful as well as a convenient strategy for investigating complex changes in patterns of gene expression (20–22). A candidate tumor suppressor ING1 has a key role as a negative regulator of cell proliferation (1, 7, 8, 11). Recently, it has been shown that ING1 is associated with HAT activity or HDAC, indicating that ING1 might be involved closely in chromatin-mediated transcriptional regulation (5, 6). However, the ING1-mediated intracellular signaling pathways have not yet been elucidated clearly. To understand the genetic basis of the ING1-induced antiproliferative effect, we used a high-density microarray of 2304 mouse cDNAs to search for differences in gene expression associated with tumorigenicity induced by the antisense *ING1* expression in NMuMG cells.

By means of the simultaneous two-color fluorescence hybridization, we have identified 16 genes (0.7% of 2304 transcripts) whose expression level was significantly increased and 9 genes (0.4% of 2304 transcripts) that were down-regulated on the overexpression of antisense *ING1*. Subsequent semiquantitative RT-PCR analysis revealed that 88 (14 of 16 genes) and 57% (5 of 9 genes) of the selected genes were confirmed to be up- and down-regulated, respectively. These results suggested that our cDNA microarray analysis was reliable. The recent cDNA microarray analysis showed that when the tumor suppressor PTEN was overproduced in PTEN-deficient cells, 2.5 and 1.8% of 4009 genes were up- and down-regulated, respectively (23).

Overexpression of ING1 by adenovirus-mediated *ING1* gene transfer to NMuMG cells significantly reduced the expression level of *cyclin B1*, *TPT1*, *DEK*, and *osteopontin* in a time-dependent manner. Among them, down-regulation of *cyclin B1* and *DEK* was extremely intriguing. DEK was identified initially as a fusion partner of the putative oncogene product, CAN, in a subtype of acute myelogenous leukemia, and the DEK-CAN fusion protein appeared to be oncogenic (24). Recently, it has been shown that DEK is a nuclear protein that binds specifically to the HIV-2 enhancer or cooperates with histone H2A/H2B to change the topology of nucleosomal DNA (25, 26). It is of great interest to note that *DEK* is highly expressed in human hepatocellular carcinoma as compared with matched normal liver tissues (27), raising a possibility that ING1-mediated alteration of *DEK* expression is involved in the development of the malignant phenotypes.

Cyclin B1, which accumulates during G_2-M phase of the cell cycle, is the regulatory subunit of the cdc2 protein kinase, and cdc2/cyclin B1 complex is required for mitotic initiation (28). In contrast, ING1 protein level starts to be increased at the late G_1, reaching a maximum in S phase followed by a significant decrease in G_2 (7). The significant reduction of *cyclin B1* expression caused by the adenovirus-mediated overproduction of ING1 was in good agreement with the cell cycle-dependent expression patterns of cyclin B1 and ING1. However, it is conceivable that the effect of overexpression of $p33^{ING1}$ on suppression of *cyclin B1* expression could be secondary to the growth inhibition. This is because that ING1 protein itself has no DNA-binding activity and that it indirectly regulates transcriptional activities of p53 or HDAC by binding to either protein. In response to genotoxic stress induced by DNA damage, p53 is activated and inhibits G_1-S transition in cells (29). In addition, p53 also plays an important role in regulating G_2-M transition. Overexpression of p53 induced G_2-M growth arrest in mammalian cells (30, 31). Recently, it has been shown that p53-dependent G_2-M arrest was associated with a reduction in the rate of *cyclin B1* transcription, followed by a decrease in intracellular cyclin B1 level (32–34). $p53^{-/-}$ mouse mammary adenocarcinomas express significantly higher levels of cyclin B1 as compared with those of $p53^{+/+}$ counterparts (34). Consistent with the notion that p53 represses the transcription from a variety of promoters lacking the consensus p53-binding site (35), *cyclin B1* promoter does not contain the putative p53-binding site (32, 33), suggesting that p53 down-regulates the transcription of *cyclin B1* without binding to the *cyclin B1* promoter. Intriguingly, ING1 was associated functionally with the HDAC1-mediated transcriptional repression (6). In addition, infection of *p53* alone induced down-regulation of *cyclin B1* expression, suggesting that endogenous ING1 cooperates with p53 to induce the down-regulation of *cyclin B1* or that p53 may also act to inhibit *cyclin B1* expression through the ING1-independent pathway. Furthermore, infection with *ING1* alone in the p53-deficient SAOS cell line also resulted in down-regulation of *cyclin B1* at 72 h, suggesting that ING1 also has a p53-independent effect on gene expression. Although the precise molecular mechanism by which ING1 represses the *cyclin B1* transcription remains to be elucidated, it could be possible that p53 cooperates with ING1/HDAC1 complex in negative regulation of *cyclin B1* expression. Our present results also supported this possibility.

Although *ING1* was mutated rarely in primary breast and ovarian cancers, as well as breast cancer cell lines, the expression level of *ING1* was reduced significantly in breast cancer cells as compared with that of normal mammary epithelial cells (9). Keyomarsi and Pardee (36) have reported that the majority of human breast cancer cell lines overexpressed cyclin B1. This inverse correlation between the expression levels of *ING1* and *cyclin B1* in breast cancer cells strongly supports the idea that ING1-mediated alteration of *cyclin B1* expression may be responsible for the uncontrolled cell growth and tumor development.

Acknowledgments

We thank Dr. I. Garkavtsev for helping on the GSE method, Drs. K. Hashimoto and S. Sugano for providing mouse cDNA clones, and Dr. S. Sakiyama for critical reading of the manuscript.

References

1. Garkavtsev, I., Kazarov, A., Gudkov, A., and Riabowol, K. Suppression of the novel growth inhibitor $p33^{ING1}$ promotes neoplastic transformation. Nat. Genet., *14:* 415–420, 1996.
2. Zeremski, M., Hill, J. E., Kwek, S. S. S., Grigorian, I. A., Gurova, K. V., Garkavtsev, I. V., Diatchenko, L., Koonin, E. V., and Gudkov, A. V. Structure and regulation of the mouse *ing1* gene. J. Biol. Chem., *274:* 32172–32181, 1999.
3. Gunduz, M., Ouchida, M., Fukushima, K., Hanafusa, H., Etani, T., Nishioka, S., Nishizaki, K., and Shimizu, K. Genomic structure of the human *ING1* gene and

tumor-specific mutations detected in head and neck squamous cell carcinomas. Cancer Res., *60:* 3143–3146, 2000.
4. Aasland, R., Gibson, T. J., and Stewart, A. F. The PHD finger: implications for chromatin-mediated transcriptional regulation. Trends Biochem. Sci., *20:* 56–59, 1995.
5. Loewith, R., Meijer, M., Lees-Miller, S. P., Riabowol, K., and Young, D. Three yeast proteins related to the human candidate tumor suppressor p33^{ING1} are associated with histone acetyltransferase activities. Mol. Cell. Biol., *20:* 3807–3816, 2000.
6. Skowyra, D., Zeremski, M., Neznanov, N., Li, M., Choi, Y., Uesugi, M., Hauser, C. A., Gu, W., Gudkov, A. V., and Qin, J. Differential association of products of alternative transcripts of the candidate tumor suppressor *ING1* with mSin3/HDAC1 transcriptional corepressor complex. J. Biol. Chem., *276:* 8734–8739, 2001.
7. Garkavtsev, I., and Riabowol, K. Extension of the replicative life span of human diploid fibroblasts by inhibition of the p33^{ING1} candidate tumor suppressor. Mol. Cell. Biol., *17:* 2014–2019, 1997.
8. Helbing, C. C., Veillette, C., Riabowol, K., Johnston, R. N., and Garkavtsev, I. A novel tumor suppressor, *ING1*, is involved in the regulation of apoptosis. Cancer Res., *57:* 1255–1258, 1997.
9. Toyama, T., Iwase, H., Watson, P., Muzik, H., Saettler, E., Magliocco, A., DiFrancesco, L., Forsyth, P., Garkavtsev, I., Kobayashi, S., and Riabowol, K. Suppression of *ING1* expression in sporadic breast cancer. Oncogene, *18:* 5187–5193, 1999.
10. Shinoura, N., Muramatsu, Y., Nishimura, M., Yoshida, Y., Saito, A., Yokoyama, T., Furukawa, T., Horii, A., Hashimoto, M., Asai, A., Kirino, T., and Hamada, H. Adenovirus-mediated transfer of p33^{ING1} with p53 drastically augments apoptosis in gliomas. Cancer Res., *59:* 5521–5528, 1999.
11. Garkavtsev, I., Grigorian, I. A., Ossovskaya, V. S., Chernov, M. V., Chumakov, P. M., and Gudkov, A. V. The candidate tumor suppressor p33^{ING1} cooperates with p53 in cell growth control. Nature (Lond.), *391:* 295–298, 1998.
12. Garkavtsev, I., Demetrick, D., and Riabowol, K. Cellular localization and chromosome mapping of a novel candidate tumor suppressor gene (*ING1*). Cytogenet. Cell Genet., *76:* 176–178, 1997.
13. Maestro, R., Piccinin, S., Doglioni, C., Gasparotto, D., Vukosavljevic, T., Sulfaro, S., Barzan, L., and Boiocchi, M. Chromosome 13q deletion mapping in head and neck squamous cell carcinomas: identification of two distinct regions of preferential loss. Cancer Res., *56:* 1146–1150, 1996.
14. Tsang, Y. S., Lo, K. W., Leung, S. F., Choi, P. H., Fong, Y., Lee, J. C., and Huang, D. P. Two distinct regions of deletion on chromosome 13q in primary nasopharyngeal carcinoma. Int. J. Cancer, *83:* 305–308, 1999.
15. Gupta, V. K., Schmidt, A. P., Pashia, M. E., Sunwoo, J. B., and Scholnick, S. B. Multiple regions of deletion on chromosome arm 13q in head-and-neck squamous cell carcinoma. Int. J. Cancer, *84:* 453–457, 1999.
16. Chen, L., Matsubara, N., Yoshino, T., Nagasaka, T., Hoshijima, N., Shirakawa, Y., Naomoto, Y., Isozaki, H., Riabowol, K., and Tanaka, N. Genetic alterations of candidate tumor suppressor *ING1* in human esophageal squamous cell cancer. Cancer Res., *61:* 4345–4349, 2001.
17. Mizuguchi, H., and Kay, M. A. Efficient construction of a recombinant adenovirus vector by an improved *in vitro* ligation method. Hum. Gene Ther., *9:* 2577–2583, 1998.
18. Mizuguchi, H., and Kay, M. A. A simple method for constructing E1- and E1/E4-deleted recombinant adenoviral vectors. Hum. Gene Ther., *10:* 2013–2017, 1999.
19. Yoshikawa, T., Nagasugi, Y., Azuma, T., Kato, M., Sugano, S., Hashimoto, K., Masuho, Y., Masa-aki, M., and Seki, N. Isolation of novel mouse genes differentially expressed in brain using cDNA microarray. Biochem. Biophys. Res. Commun., *275:* 532–537, 2000.
20. Schena, M., Shalon, D., Davis, R. W., and Brown, P. O. Quantitative monitoring of gene expression patterns with a complementary DNA microarray. Science (Wash. DC), *270:* 467–470, 1995.
21. DeRisi, J., Penland, L., Brown, P. O., Bittner, M. L., Meltzer, P. S., Ray, M., Chen, Y., Su, Y. A., and Trent, J. M. Use of a cDNA microarray to analyze gene expression patterns in human cancer. Nat. Genet., *14:* 457–460, 1996.
22. Wang, K., Gan, L., Jeffery, E., Gayle, M., Gown, A. M., Skelly, M., Nelson, P. S., Ng, W. V., Schummer, M., Hood, L., and Mulligan, J. Monitoring gene expression profile changes in dvarian carcinomas using cDNA microarray. Gene, *229:* 101–108, 1999.
23. Matsushima-Nishi, M., Unoki, M., Ono, K., Tsunoda, T., Minaguchi, T., Kuramoto, H., Nishida, M., Satoh, T., Tanaka, T., and Nakamura, Y. Growth and gene expression profile analysis of endometrial cancer cells expressing exogenous PTEN. Cancer Res., *61:* 3741–3749, 2001.
24. von Lindern, M., Fornerod, M., van Baal, S., Jaegle, M., de Wit, T., Buijs, A., and Grosveld, G. The translocation (6;9), associated with a specific subtype of acute myeloid leukemia, results in the fusion of two genes, dek and can, and the expression of a chimeric, leukemia-specific dek-can mRNA. Mol. Cell. Biol., *12:* 1687–1697, 1992.
25. Fu, G. K., Grosveld, G., and Markovitz, D. M. DEK, an autoantigen involved in a chromosomal translocation in acute myelogenous leukemia, binds to the HIV-2 enhancer. Proc. Natl. Acad. Sci. USA, *94:* 1811–1815, 1997.
26. Alexiadis, V., Waldmann, T., Andersen, J., Mann, M., Nippers, R., and Gruss, C. The protein encoded by the proto-oncogene DEK changes the topology of chromatin and reduces the efficiency of DNA replication in a chromatin-specific manner. Genes Dev., *14:* 1308–1312, 2000.
27. Kondoh, N., Wakatsuki, T., Ryo, A., Hada, A., Aihara, T., Horiuchi, S., Goseki, N., Matsubara, O., Takenaka, K., Shichita, M., Tanaka, K., Shuda, M., and Yamamoto, M. Identification and characterization of genes associated with human hepatocellular carcinogenesis. Cancer Res., *59:* 4990–4996, 1999.
28. Elledge, S. J. Cell cycle checkpoints: preventing an identity crisis. Science (Wash. DC), *274:* 1664–1672, 1996.
29. Levine, A. J. p53, the cellular gatekeeper for growth and division. Cell, *88:* 323–331, 1997.
30. Agarwal, M. L., Agarwal, A., Taylor, W. R., and Stark, G. R. p53 controls both the G2/M and the G1 cell cycle checkpoints and mediates reversible growth arrest in human fibroblasts. Proc. Natl. Acad. Sci. USA, *92:* 8493–8497, 1995.
31. Stewart, N., Hicks, G. G., Paraskevas, F., and Mowat, M. Evidence for a second cell cycle block at G2/M by p53. Oncogene, *10:* 109–115, 1995.
32. Sugrue, M. M., Shin, D. Y., Lee, S. W., and Aaronson, S. A. Wild-type p53 triggers a rapid senescence program in human tumor cells lacking functional p53. Proc. Natl. Acad. Sci. USA, *94:* 9648–9653, 1997.
33. Taylor, W. R., DePrimo, S. E., Agarwal, A., Agarwal, M. L., Schonthal, A. H., Katula, K. S., and Stark, G. R. Mechanisms of G2 arrest in response to overexpression of p53. Mol. Biol. Cell, *10:* 3607–3622, 1999.
34. Cui, X-S., and Donehower, L. A. Differential gene expression in mouse mammary adenocarcinomas in the presence and absence of wild type p53. Oncogene, *19:* 5988–5996, 2000.
35. Mack, D. H., Vartikar, J., Pipas, J. M., and Laimins, L. A. Specific repression of TATA-mediated but not initiator-mediated transcription by wild-type p53. Nature (Lond.), *363:* 281–283, 1993.
36. Keyomarsi, K., and Pardee, A. B. Redundant cyclin overexpression and gene amplification in breast cancer cells. Proc. Natl. Acad. Sci. USA, *90:* 1112–1116, 1993.

Identification of the p33^{ING1}-regulated Genes that Include *Cyclin B1* and Proto-oncogene *DEK* by Using cDNA Microarray in a Mouse Mammary Epithelial Cell Line NMuMG

Masato Takahashi, Naohiko Seki, Toshinori Ozaki, et al.

Cancer Res 2002;62:2203-2209.